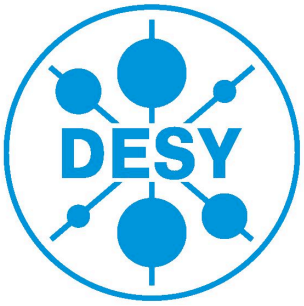

SUSY discovery scenarios with the single lepton final state at LHC and HL-LHC in CMS experiment.

Nadezda Chernyavskaya[1,2]

[1] Institute for Theoretical and Experimental Physics, Russia

[2]Moscow Institute of Physics and Technology, Russia

Supervisors:

Batool Safarzadeh Samani

Isabell Melzer-Pellmann

September 5, 2014

Abstract

In this report we discuss three full SUSY natural models and their possible discovery in the inclusive search with a single lepton final state at LHC and HL-LHC in the CMS experiment. In this analysis S_T and L_P are chosen as discriminating variables. Different pileup scenarios: 140PU and 50 PU are considered. Six search bins are proposed to reach the discovery sensitivity for the integrated luminosity of 300 fb^{-1}. The discovery significance as a function of background uncertainty is evaluated. As result we present the expected sensitivity as a function of integrated luminosity.

Contents

1 Introduction

1.1 Introduction to SUSY

The standard model (SM) is a successful theory which provides a description of three forces of nature: electromagnetic, weak and strong. It not only explains much of what is observed experimentally, but even makes predicts new particles. In 2012, when Higgs particle was found at Large Hadron Collider (LHC), it was the triumph of the SM theory. However there are several open questions that can't be explained by the SM:

- Non-zero neutrino masses
- Huge radiative corrections to the Higgs mass.
- We have no hints about dark matter and dark energy.
- The SM does not include gravity.
- Electromagnetic, weak and strong forces can't be unified at Planck scale.

The Standard Model is supposed to be a low-energy effective theory. Nowadays many searches of physics beyond the standard model are performed, one of the most promising theories is Supersymmetry (SUSY). SUSY is very appealing, because it postulates a symmetry that hidden at low energy scales. It predicts that every SM particle has a partner with a spin differing by 1/2. A new transformation operator Q can be introduced, that gives us the symmetry between bosons and fermions.

$$Q|fermion\rangle = |boson\rangle$$
$$Q|boson\rangle = |fermion\rangle$$

Supersymetric partners of SM particles are called sparticles. The partner of quark is called squark (for example top quark: t $\rightarrow \widetilde{t}_1$ or $\widetilde{t}_2$). A new quantum number is introduced, R-parity is defined as follows: R = $(-1)^{2s+3B+L}$, where s is the spin of a particle, B the baryon number and L the lepton number. For all SM particles R = 1, for sparticles R = -1.
The minimal supersymmetric extension of the SM is the *Minimal Supersymetric Standard Model* (MSSM). Since partners of SM particles haven't been observed yet, the symmetry between SM and SUSY particles must be broken and mass range of sparticles is shifted to higher masses. SUSY cannot predict masses of new particles, thus the theory has a huge number of free parameters. the MSSM has 125 free parameters. In order to constrain some parameters, a few assumptions

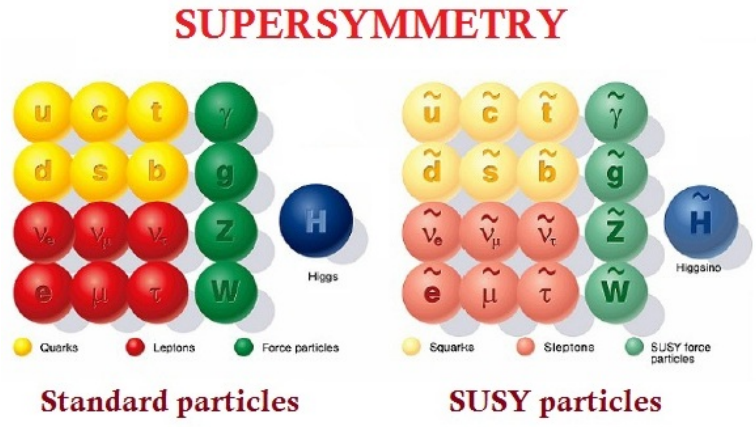

Figure 1: Schematic spectrum of SM particles and their partners.

are made to simplify the theory: phemenological MSSM (pMSSM) and constrained MSSM (CMSSM) [1]. These theories set the minimal number of free parameters to get consistent theory, having R-parity conserved or not. Note that if R-parity is conserved, the sparticles can only be produced in pairs. In Fig 1, a schematic spectrum of SM particles and their partners is presented. After electro-weak symmetry breaking new mass eigenstates exist: three neutral Higgs bosons (h_0, the one with the lightest mass, that supposed to be discovered at LHC in 2012, H_0 and A_0), two charged Higgs bosons ($H^{\pm}$), charged and neutral binos (partners of Z-boson) and winos (partners of W-boson) and to complete the list, gluino and gravitino are introduced. Left- and right-handed fermions have different SUSY partners, that can mix in f_1 or f_2 states with different masses. Winos, binos and higgsinos can also mix in new states and give four neutralinos ($\widetilde{\chi}^0_{1,2,3,4}$) and four charginos ($\widetilde{\chi}^{\pm}_{1,2}$). If R-partity is conserved, the Lightest Supersumetric Particle (LSP) must be stable. LSP is neutral and weakly interacting current, in most models it is $\widetilde{\chi}^0_1$ or gravitino. The stable LSP goes through detector without being detected and we expect to reconstruct more missing energy in events with SUSY particles production.

Why can SUSY solve the problems that we face with SM?

- Neutrino masses are expected in SUSY.
- Corrections to the Higgs mass can be canceled by scalar partner particles.
- The LSP can be perfect dark matter candidate.
- Gravity can be included in SUSY theory.
- Unification of forces at 10^{16} GeV.

1.2 SUSY at LHC and HL-LHC

SUSY searches have been performed for the last 20 years, but we have no hint of existing SUSY particles yet. However, some regions of phase space were excluded in the previous LHC runs at 7 and 8 TeV [2, 3]. In 2015 the LHC will run at center-of-mass energy of 13 TeV and the center-of-mass energy will increase to 14 TeV in the following years. Until 2023, the LHC will increase its integrated luminosity to $300 fb^{-1}$ compared to integrated luminosity of $19.5 fb^{-1}$ after 8 TeV LHC run in 2012. It is also planned that until 2035 the High-Luminosity LHC (HL-LHC) can deliver up to $3000 fb^{-1}$. As the new phase space region is open to us, we expect to see the signals of SUSY particles. In this work we perfom an analysis for LHC run at $\sqrt{s} = 14$ TeV.

Since we have too many free parameters in the theory, masses of sparticles, branching ratios and decay modes differ significantly in different SUSY full models with fixed parameters. Before the detector is upgraded to higher luminosity, our goal is to investigate several possible SUSY scenarios with different mass spectra and decay modes in order to understand how we can discover SUSY production if such a scenario takes place in reality. The idea is to generate the data for each model, then run it through a detector simulation package and analyse the data like we do when we have real collisions at LHC. We know the SM background processes well and by comparing signal samples with background samples we can conclude whether we can make a discovery at the CMS experiment assuming a particular model.

In this paper we will examine three full natural models NM1, NM2, NM3 on possible discovery in CMS experiment at LHC and HL-LHC. These three models have different LSP ($\widetilde{\chi}_1^0$) composition, it can be either Bino-like or Higgsino-like. Depending on it the decay modes differ noticeably which will be discussed in this report.

We use three generated signal samples. These models are calculated using generators packages such as SUSPECT 2.41/2.43 or SOFTSUSY 3.4.0 in combination with SUSY-HIT 1.3b/3.4. The resulting SLHA files are processed with MADEVENT, and hadronized with PYTHIA 6.4. The resulting files ran through detector simulation package DELPHES 3.0.10, a framework for a fast simulation of a collider experiments. In this framework all parts of the CMS detector are simulated, taking into account the magnetic field, the granularity of the calorimeters and the detectors resolution. More on the CMS detector in Sec. 2.

When we upgrade the collider to higher energies and luminosities, we expect to have in addtition to the hard interaction many simultaneous pp collisions called pileup. In this work we will consider two pileup scenarios: 50PU and 140PU. We

use samples from PhaseII 140PU ProdJul28 sample for 140PU and PhaseI 50PU ProdAug6 for 50PU. For each model we will discuss the discovery sensitivity depending on the integrated luminosity.

2 CMS experiment

The Compact Muon Solenoid (CMS) is a general-purpose detector at the Large Hadron Collider (LHC). It is designed to investigate a broad range of physics, including physics beyond the SM. The detector is 21 m long, 15 m wide and 15 m high. In Fig. 2 a transverse slice of the detector is shown. The detector has an onion-like structure. The main feature of the detector is a huge solenoid magnet, that generates field of 3.8 T. Within the volume of the magnetic field essential parts for detecting particles of different types are embedded:

- Silicon pixel detector, allowing to measure the vertex position and paths of particles with great precision.
- Strip tracker allows to reconstruct tracks of particles and measure their momenta.
- Electromagnetic calorimeter, made of lead tungstate, measures energy of electrons and photons.
- Hadron calorimeter to detect and measure energy of hadrons. It uses layers of absorber and scintillator material that produces a rapid light pulse when a particle passes through.
- Muon detector consists of multiple layers, measuring the position of the particle in each layer can provide momentum of muons.

In the CMS experiment the interaction point is the origin of the coordinate system. The x-axis points to the center of the LHC ring. The y-axis goes vertically upwards. The z-axis lies in the direction of the nominal proton beam. The polar angle θ is measured from the positive z-axis, and the azimuthal angle ϕ is measured in x-y plane.

3 Natural models NM1, NM2, NM3

In this section we discuss three full natural models, which differ mostly by mass hierarchy and decay modes. In all three models gluino mass is set to 1.69 TeV and the third generation squarks are the lightest. Top squark $\widetilde{t}_1$ and bottom squark $\widetilde{b}_1$ are in the region of LHC reach, while $\widetilde{t}_2$, $\widetilde{b}_2$ and other generation squarks are

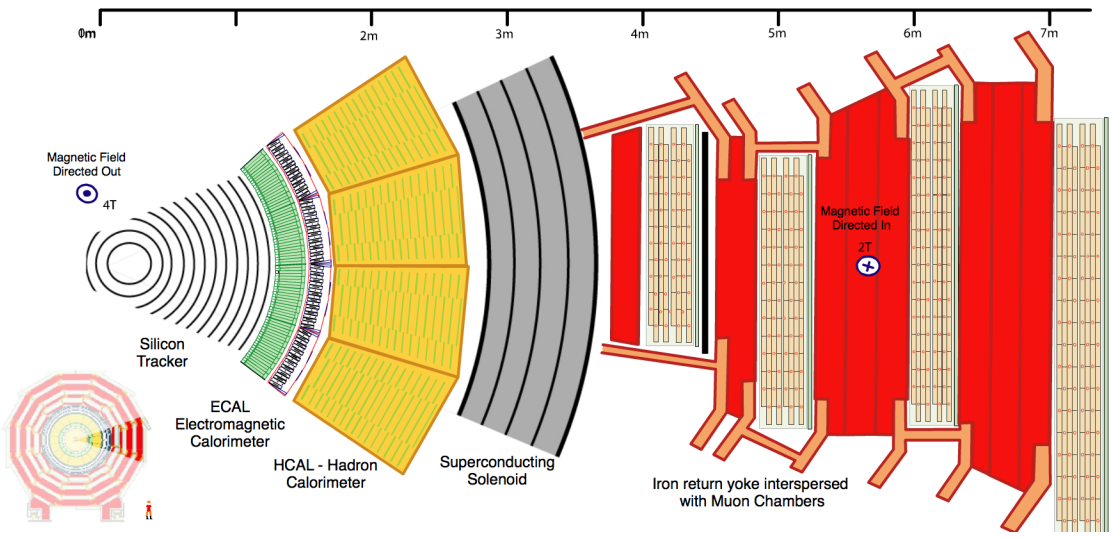

Figure 2: Transverse Slice of the Compact Muon Solenoid (CMS) Detector.

out of LHC reach. Squarks can be produced either in pairs in gluino decay, or in direct pair production. However direct gluino production is dominant in these models and is 99%. In this analysis we are interested only in gluino production. Since gluionos are produced in pairs, one can observe three different channels, as shown in Fig. 3. Branching ratios for gluino decays in all models are equal and following: $\mathrm{BR}(\widetilde{g} \to \widetilde{t}_1 t) = 60\%$, $\mathrm{BR}(\widetilde{g} \to \widetilde{b}_1 b) = 40\%$. The mass spectrum and important branching ratios for all models are presented in Tab. 2 and in Tab. 1 correspondingly.

The NM1 model has a Bino-like $\widetilde{\chi}_1^0$ with a mass of 419 GeV, and top squark with a mass of 1.08 TeV. The NM1 model has long decay chain, with relatively small sneutrino mass, that allows it to be produced at LHC resulting in large missing energy. A lepton can originate not only from W decay, but also from $\widetilde{\chi_1^\pm} \to \widetilde{\nu} l^\pm$ decay, that leads to high lepton multiplicity. This is the feature of the NM1 model, in other models we do not have such a decay mode and leptons mostly originate from W decay. A cross section for this model is 0.1 pb.

The NM2 is a model with Bino-like $\widetilde{\chi}_1^0$ and high-mass sleptons. We expect the highest jet multiplicity due to production of two $W^\pm$. A cross section is 0.07 pb.

In the NM3 the LSP is a Higgsino-like and the mass difference between $\widetilde{\chi_2^0}$ and $\widetilde{\chi_1^\pm}$ is only 7 GeV. In this model the top and bottom squarks cannot be separated from each other, as the top quark mainly decays to $\widetilde{\chi_2^0}$, while the bottom squark

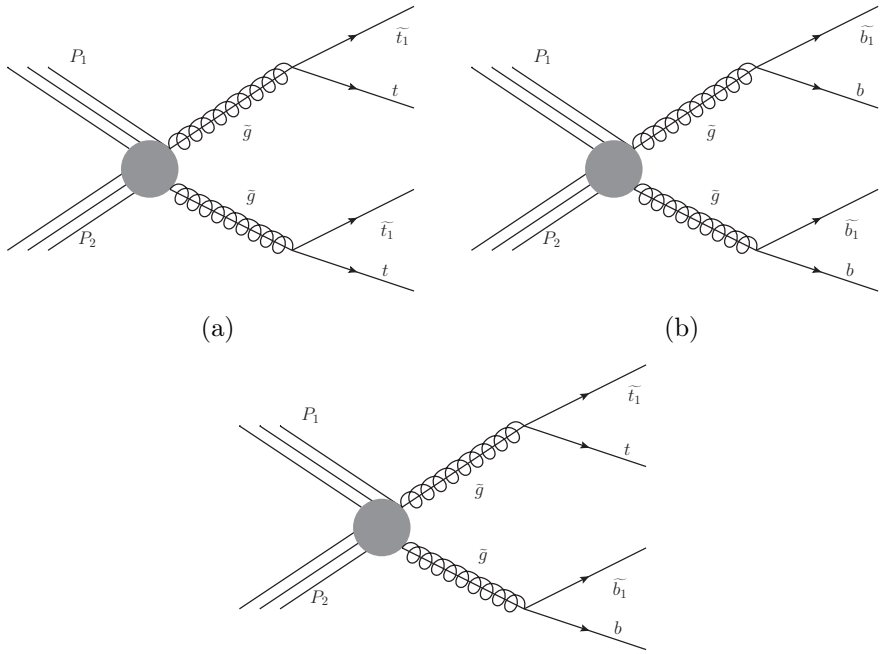

Figure 3: Three possible gluiono pair production and decay modes at LHC.

to top and $\widetilde{\chi_1^{\pm}}$. Both charginos decay to $\widetilde{\chi_1^0}$ and soft jets or sleptons. However, this signature gives us a hint for the presence of the third-generation squarks. A cross section for this model is 1.96 pb.

4 Inclusive search in single lepton final state with $\mathbf{L_P}$ and $\mathbf{S_T}$ variables.

In this section we investigate the single lepton final state using as discriminating variables S_T and L_P. As mentioned in Sec. 3 we expect high jet multiplicity, large missing energy from undetected LSP and neutrinos, hard jets (with high p_T). In this analysis we will use the measure of hadronic activity H_T, missing transverse energy $E_T^{\text{miss}}$and kinematic variable L_P, which are defined as follows:

$$E_T^{\text{miss}} = |-\sum_{all\ particles} \vec{p_T}|, \quad H_T = \sum_{all\ jets} |\vec{p_T}|, \quad S_T = E_T^{\text{miss}} + p_T(l)$$

$$L_P = \frac{\vec{P_T}(l)\vec{P_T}(W)}{P_T(W)^2} = \frac{P_T(l)}{P_T(W)}\cos(\Delta\phi)$$

Table 1: Branching ratios in natural models.

Decay modes					
NM1		**NM2**		**NM3**	
$\widetilde{b_1} \to \widetilde{\chi_2^{\pm}} t$	49%	$\widetilde{b_1} \to \widetilde{\chi_2^{\pm}} t$	48%	$\widetilde{b_1} \to \widetilde{\chi_1^{\pm}} t$	80%,
$\widetilde{t_1} \to \widetilde{\chi_4^0} t$	30%	$\widetilde{t_1} \to \widetilde{\chi_4^0} t$	30%	$\widetilde{t_1} \to \widetilde{\chi_2^0} t$	41%,
$\widetilde{\chi_4^0} \to \widetilde{\chi_1^{\pm}} W^{\pm}$	16%	$\widetilde{\chi_4^0} \to \widetilde{\chi_1^{\pm}} W^{\pm}$	36%	$\widetilde{\chi_2^0} \to \widetilde{\chi_1^0} q\bar{q}$	35%.
$\underline{\widetilde{\chi_1^{\pm}} \to \widetilde{\nu} l^{\pm}}$	58%	$\widetilde{\chi_1^{\pm}} \to \widetilde{\chi_1^0} W^{\pm}$	100%		

Table 2: Mass spectrum in natural models

Mass spectrum		
NM1	**NM2**	**NM3**
$m(\widetilde{g}) = 1.69$ TeV	$m(\widetilde{g}) = 1.69$ TeV	$m(\widetilde{g}) = 1.69$ TeV
$m(\widetilde{t_1}) = 1.08$ TeV	$m(\widetilde{t_1}) = 1.08$ TeV	$m(\widetilde{t_1}) = 1.14$ TeV
$m(\widetilde{b_1}) = 1.18$ TeV	$m(\widetilde{b_1}) = 1.18$ TeV	$m(\widetilde{b_1}) = 1.16$ TeV
$m(\widetilde{\chi_0^1}) = 419$ GeV	$m(\widetilde{\chi_0^1}) = 199$ GeV	$m(\widetilde{\chi_0^1}) = 195$ GeV
$m(\widetilde{\chi_4^0}) = 644$ GeV	$\underline{m(\widetilde{\chi_4^0}) = 656 \text{ GeV}}$	$m(\widetilde{\chi_4^0}) = 837$ GeV
$m(\widetilde{\chi_1^{\pm}}) = 512$ GeV	$\underline{m(\widetilde{\chi_1^{\pm}}) = 534 \text{ GeV}}$	$m(\widetilde{\chi_1^{\pm}}) = 201$ GeV
$\underline{m(\widetilde{\nu}) = 425 \text{ GeV}}$	$m(\widetilde{\nu}) = 3$ TeV	$m(\widetilde{\nu}) = 3$ TeV

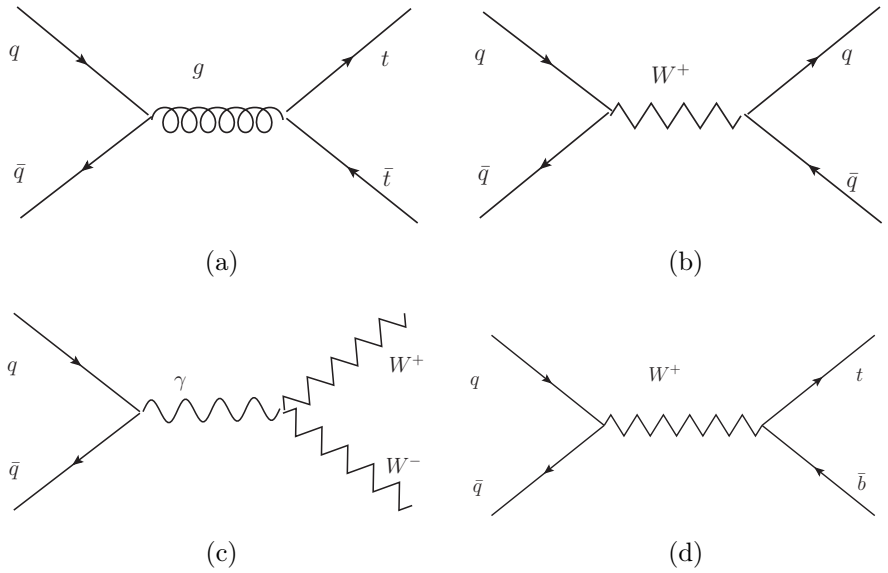

Figure 4: Feynman diagrams for background events: (a) - t$\bar{t}$, (b) - Boson + jets, (c) - DiBoson, (d) - single top+ jets

$$P_T(W) = \sqrt{(E_T^{\text{miss}})^2 + P_T^2(l) + 2 \cdot P_T(l) \cdot E_T^{\text{miss}} \cdot \cos(\Delta\phi(l, E_T^{\text{miss}}))}$$

$$\phi(W) = atan\frac{P_y}{P_x} = atan\frac{P_y(\nu) + P_y(l)}{P_x(\nu) + P_x(l)}$$

where $\vec{P_T}(W)$ and $\vec{P_T}(l)$ are the transverse momenta of the W boson and the charged lepton respectively, and $\Delta\phi(W, l)$ is the azimuthal angle between the W boson and the charged lepton. In SUSY decays not only neutrinos contribute to the missing transverse energy, but also LSPs. Thus the W boson p_T which is calculated as a vectorial sum of the transverse momenta of the charged lepton and the missing transverse energy is expected to be higher than in SM processes. L_P gives us a tool to separate SUSY signals from SM background processes.

There are four main SM background processes to this SUSY search: t$\bar{t}$, Boson + jets, DiBoson, single top+ jets. In Fig. 4 the Feynman diagrams of one possible channel for each background are represented. Contributions to this final state from other SM processes are negligible.

4.1 Preselection

In Fig. 5 the lepton multiplicity is shown. As we had expected NM1 sample has the highest lepton multiplicity. We require a single electron or muon with $p_T >$ 10 GeV and $|\eta_\mu| < 2.1$ and $|\eta_{el}| < 2.4$, where $\eta = -ln[tan\frac{\theta}{2}]$. In order to exclude leptons originating from heavy-quark decays, we need to require the lepton to be isolated. The relative isolation of the lepton is defined as $I_{rel} = \frac{\sum(E_T+p_T)}{p_T(lep)}$, where the sum is over the transverse energy E_T (as measured in the electromagnetic and hadron calorimeters) and the transverse momentum p_T (as measured in the silicon tracker) of all reconstructed objects within this cone of size $\Delta R < 0.3$, excluding the track itself. The isolation cone is defined as $\Delta R = \sqrt{(\Delta\eta)^2 + (\Delta\phi)^2}$. The lepton is required to be isolated with $I_{rel} < 0.15$. Events with more than one lepton or with an only one lepton but not passing loose preselection criteria are rejected.

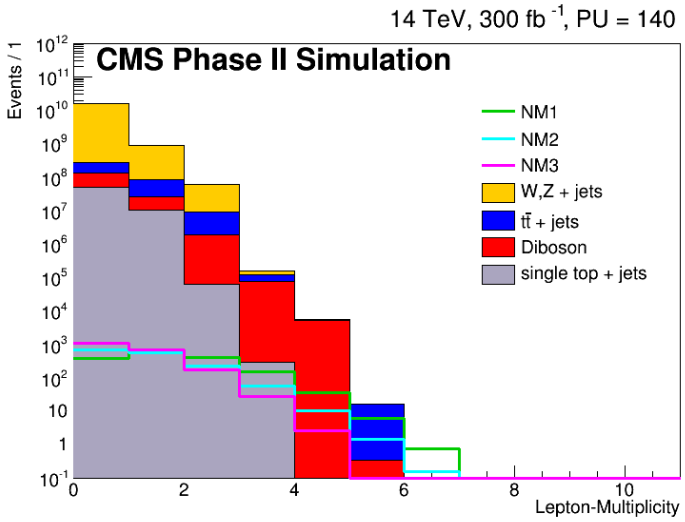

Figure 5: Lepton multiplicity with $p_T > 10$ GeV and $|\eta_\mu| < 2.1$ and $|\eta_{el}| < 2.4$. The distribution is shown for PU = 140.

We require jets with $p_T(jet) > 40$ GeV, $|\eta(jet)| < 2.5$ in order to suppress noise from calorimeters. Only the jets that are spatially separated from the selected lepton $\Delta R > 0.3$ pass the selection. Fig. 6 shows the jet and b-jet multiplicity distributions after applying the single lepton requirement and $p_T(jet) > 40$ GeV, $|\eta(jet)| < 2.5$. One can see that jet- and b-jet- multiplicity are much higher in signal samples than in backgrounds. To suppress SM background we require at least six jets in an event.

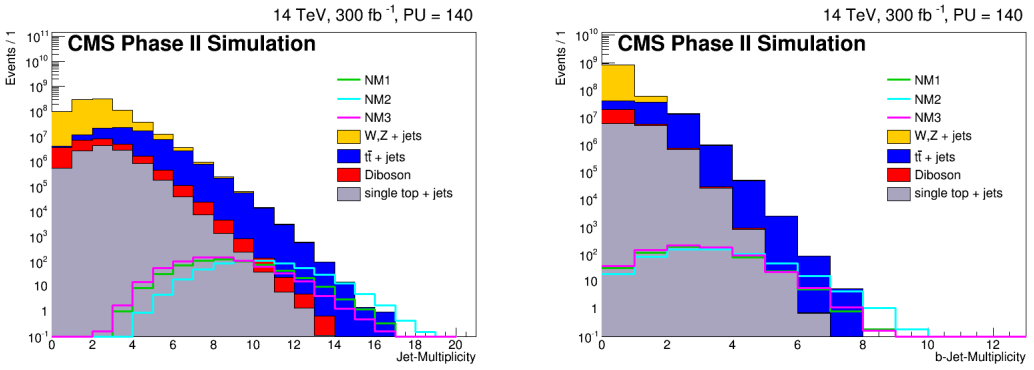

(a) (b)

Figure 6: Jet (a) and b-jet (b) multiplicity distribution after applying the single lepton requirement and $p_T(jet) > 40$ GeV, $|\eta(jet)| < 2.5$ for SM backgrounds and NM1, NM2, NM3 models. The distributions are shown for PU = 140.

Next step to separate signal events from SM backgrounds is to require hard(with high p_T) leading jets. The leading and next to leading jet p_T are shown in Fig. 7. We select events with leading jet $p_T > 300$ GeV, second leading jet $p_T > 200$ GeV, third leading jet $p_T > 75$ GeV.

Summarizing the preselection done:

- Single electron or muon with $p_T > 10$ GeV and $|\eta_\mu| < 2.1$ and $|\eta_{el}| < 2.4$. $I_{rel} < 0.15$.
- ≥ 6 jets with $p_T > 40$ GeV and $|\eta| < 2.5$.
- Leading jet $p_T > 300$ GeV, second leading jet $p_T > 200$ GeV, third leading jet $p_T > 75$ GeV.

4.2 Event Selection

As it was discussed in Sec.1.1 and Sec.3 SUSY scenarios have large missing transverse energy, due to LSP and sneutrinos, that escape detection. Signal samples have large hadronic activity, due to high jet multiplicity and jets with p_T higher than in SM processes. We can use these SUSY features to distinguish signal from background. The event selection is done as follows:

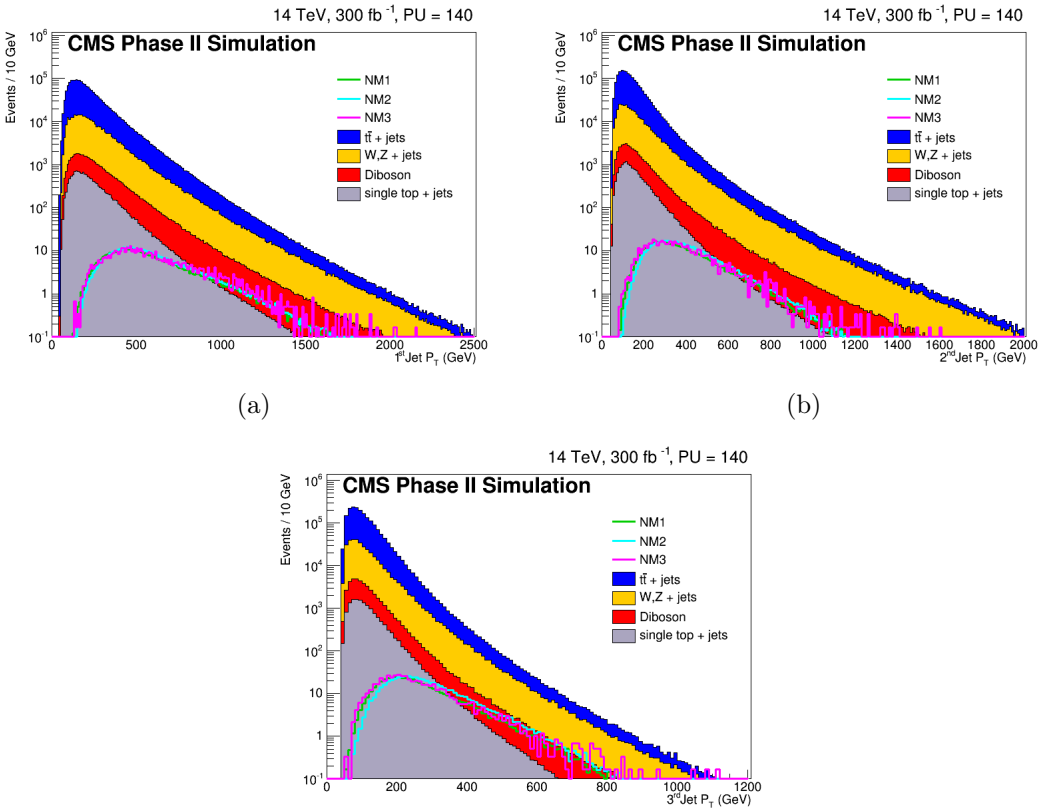

(a) (b)

(c)

Figure 7: 1^{st} leading jet p_T (a) and 2^{nd} leading jet p_T (b) distributions after applying the single lepton requirement and $p_T(jet) > 40$ GeV, $|\eta(jet)| < 2.5$ for SM backgrounds and NM1, NM2, NM3 models. The distributions are shown for PU = 140.

- H_T >1500 GeV, which suppresses the background contribution by an order of two.
- $|L_P| < 0.2$ supresses the SM background, that passes the H_T requirement.
- To increase sensitivity, we define six different search bins using the S_T threshold and b-jet multiplicity as shown in Tab. 3. For b-jets we use the medium working point.

In all search bins the main background comes from $t\bar{t}$ events, while the contribution from other processes is very small. Fig. 8 shows the H_T distribution after event preselection and the S_T distribution after applying the H_T requirement. Both distributions are made for the signal regions with number of b-jets ≥ 3. In Fig. 9 the

L_P distribution is shown for the first search bin. After applying the L_P requirement one can observe an excess of events, as shown in Fig. 10

Table 3: Selection requirements for the six signal regions (SR).

SR	Selection	SR	Selection
1	≥ 3 b-jets, $S_T > 600$ GeV	4	≥ 4 b-jets, $S_T > 600$GeV
2	≥ 3 b-jets, $S_T > 700$ GeV	5	≥ 4 b-jets, $S_T > 700$GeV
3	≥ 3 b-jets, $S_T > 800$ GeV	6	≥ 4 b-jets, $S_T > 800$GeV

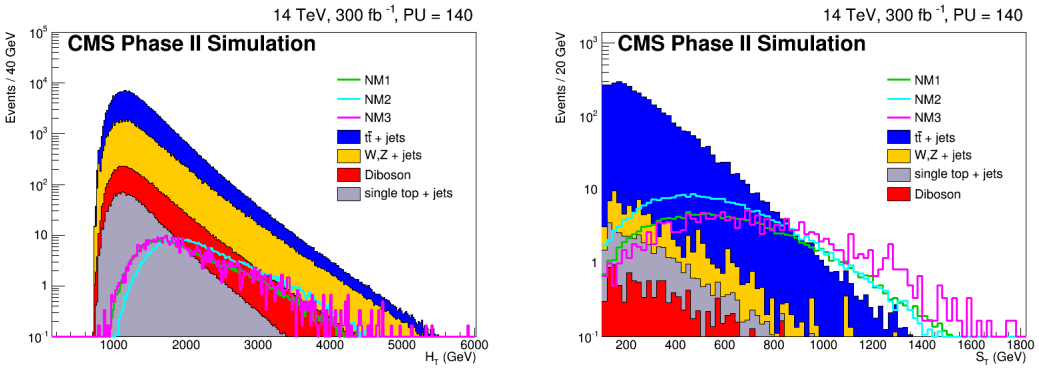

(a) (b)

Figure 8: H_T distibution after event preselection and S_T distribution after applying $H_T > 1500$ GeV. The distributions are shown for SM backgrounds and NM1, NM2, NM3 models, PU = 140.

4.3 Results

The signal and background yields for each search bin are summarized in Tab. 4. One can see that in the last search bins there are almost no backfround events left, however statistics becomes lower. The final event yields are compared between two different pileup scenarios: 50PU and 140PU with the same integrated luminosity. From the comparison of these two pileup scenarios in Tab. 4 we can say that the analysis is not pileup dependent.
To conclude whether we are sensitive to a signal, we need to look at the significance (expected sensitivity). Significance $Z = \frac{x-\mu}{\sigma}$, where μ is the mean , σ is the

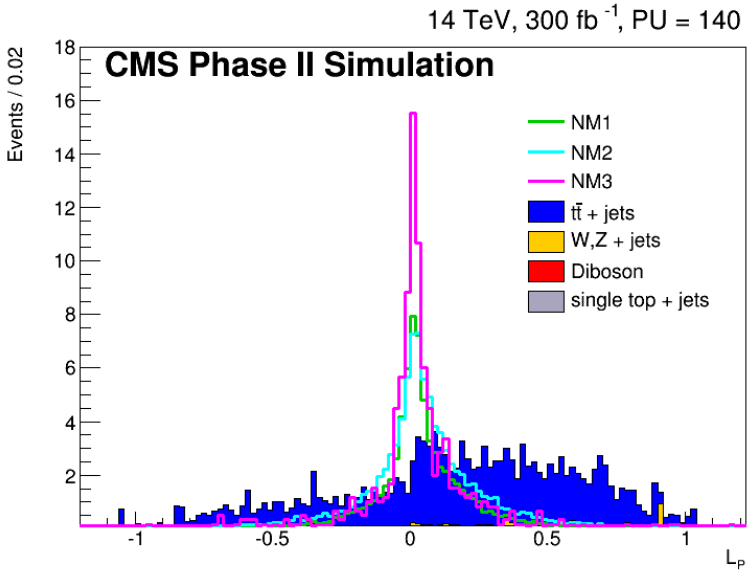

Figure 9: L_P distribution for the first search bin for SM backgrounds and NM1, NM2, NM3 models. The distribution is shown for PU = 140.

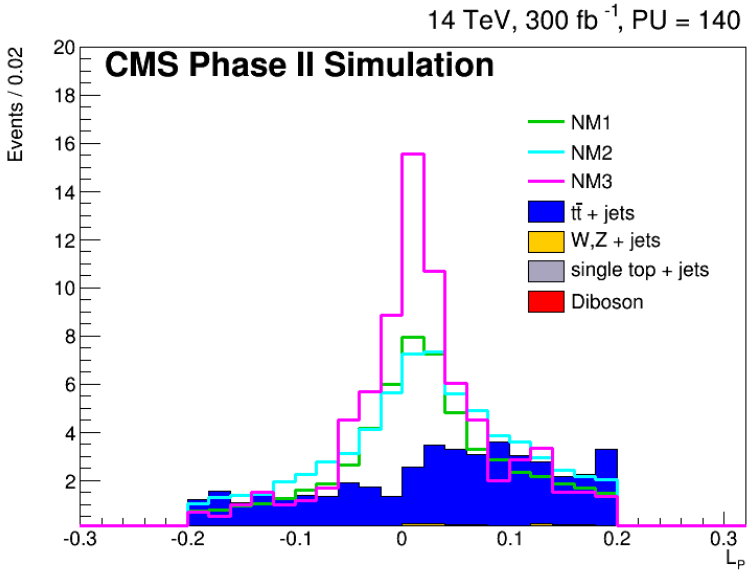

Figure 10: L_P distribution after the L_P requirement for the first search bin for SM backgrounds and NM1, NM2, NM3 models. The distribution is shown for PU = 140.

standard deviation. In high energy physics (HEP) most of the time the p-value is calculated and then it is translated in a significance. p-value - is a probability to obtain a test-statistic result (assuming that the null-hypothesis is true) close to the one that was actually observed.

$$p = P(S \geq observed \mid assume\ only\ background),$$
$$Z = \Phi^{-1}(p)$$

where $\Phi(z)$ is the distribution that is used. In this analysis we compare two different methods of the significance calculation. The first method is based on binomial probability p-value, "BinomialObsZ" method [4]. The second method is based on simple "signal to noise ratio" taking into account background a systematic uncertainty $Z = \frac{S}{B+(\delta B)^2}$, where S - number of signal events, B - number of background event, δB - background systematic uncertainty. In Fig. 11 one can find significance as a function of systematic uncertainty for these two methods . The significance calculated using "Signal to noise" is too high and cannot describe the reality well. In this paper we will use more conservative and reliable method "BinomialObsZ".

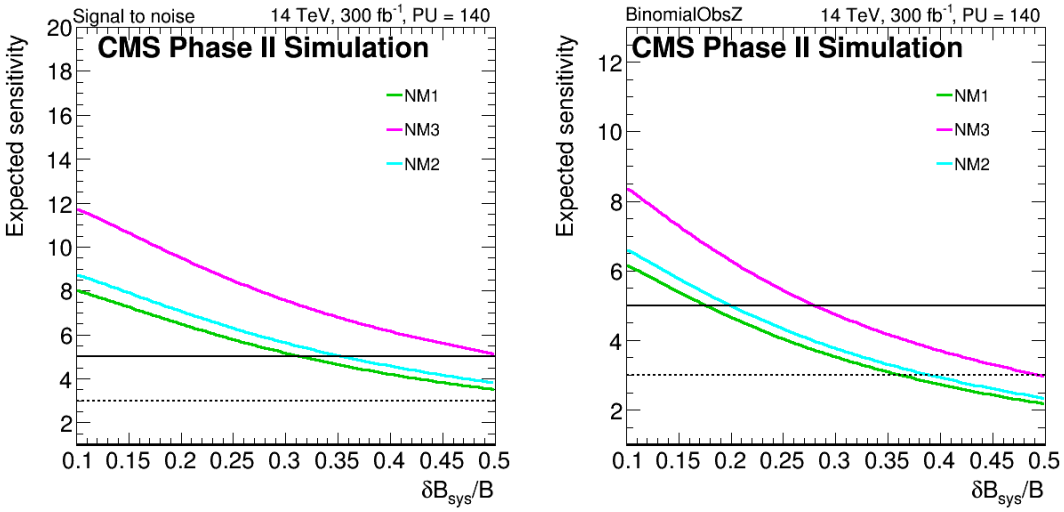

(a) (b)

Figure 11: Expected sensitivity as a function of systematic uncertainty for the second search bin ($\geq$ 3 b-jets, $S_T > 700$ GeV) for two significance calculation methods: "Signal to noise" (a), BinomialObsZ (b).

We assume a systematic uncertainty on the background prediction of the order of 20-30%, which is consistent with the 25% uncertainty from previous the 8 TeV single lepton analysis [3]. In Fig. 12 the significance dependence on the background

uncertainty is shown for two search bins with the best sensitivity for the integrated luminosity 300 fb^{-1}. We can discover NM3 with uncertainty less or equal 50%, NM2 with less than 45% and NM1 less than 35%. In Fig. 13 the significance dependence on the background uncertainty is shown for the integrated luminosity 3000 fb^{-1} for the same search bins. Even with the background uncertainty greater than 50% we still can discover the signal. This result gives us hope to see the signal in the nearest future. The expected sensitivity as a function of integrated luminosity is demonstrated in Fig. 14 for 20% and in Fig. 15 for 30% background uncertainty. We also assume very conservative background uncertainty in 50%, as shown in Fig. 16. It was investigated that NM1 is discoverable with the integrated luminosity 700 fb^{-1}, NM2 with 400 fb^{-1} and NM3 already with 200 fb^{-1}.

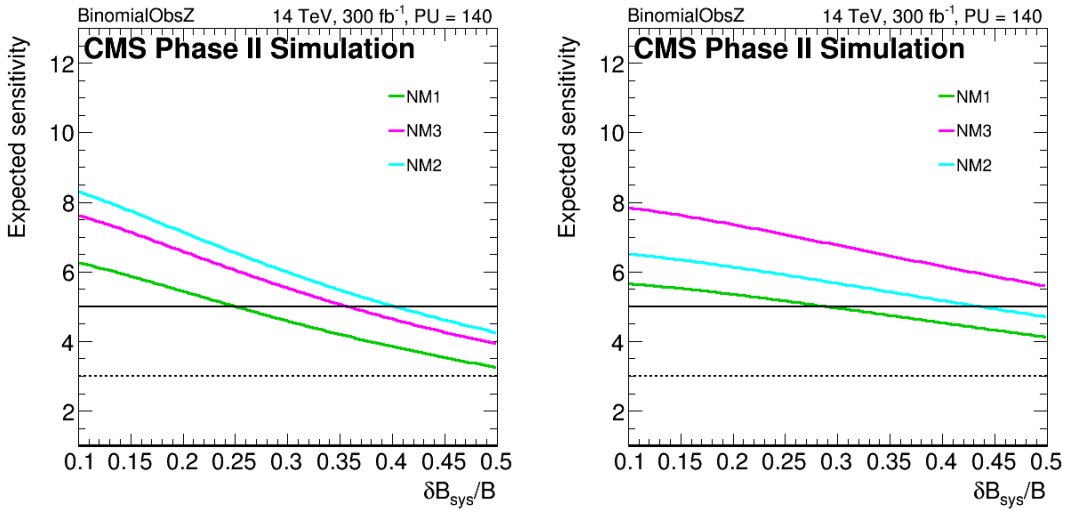

(a) (b)

Figure 12: Expected sensitivity as a function of systematic uncertainty for two search bins : ≥ 4 b-jets, $S_T > 600$ GeV (a), ≥ 4 b-jets, $S_T > 800$ GeV (b).

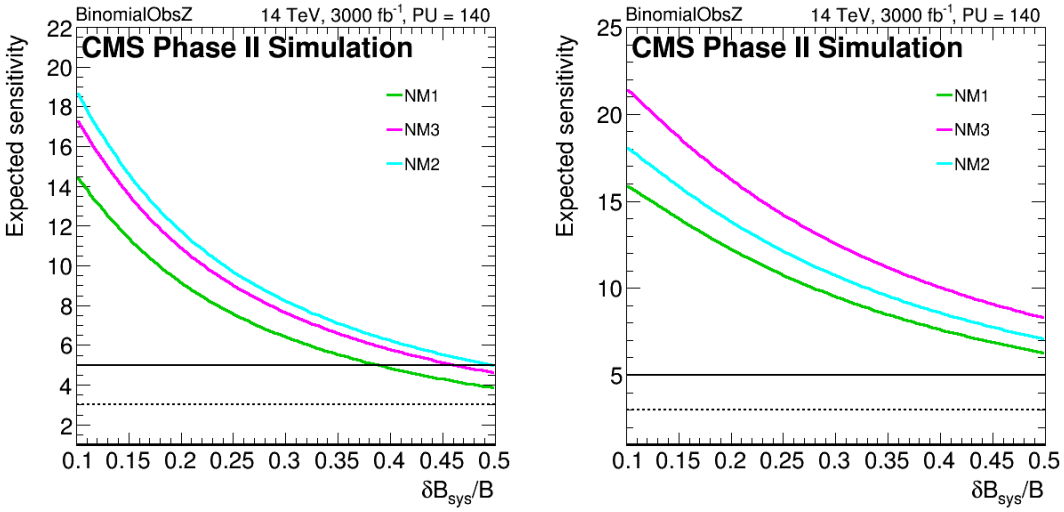

(a) (b)

Figure 13: Expected sensitivity as a function of systematic uncertainty for two search bins : ≥ 4 b-jets, $S_T > 600$ GeV (a), ≥ 4 b-jets, $S_T > 800$ GeV (b) for the integrated luminosisty 3000 fb^{-1}.

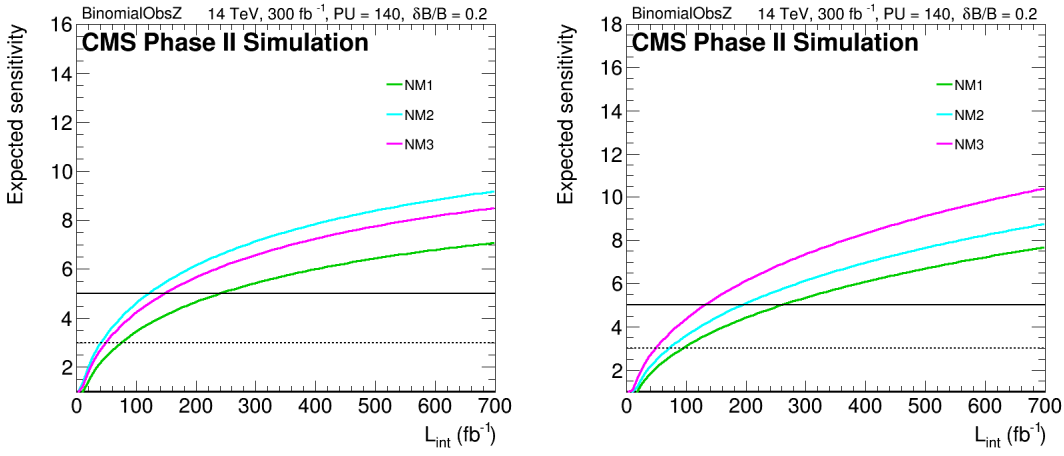

(a) (b)

Figure 14: Expected sensitivity as a function of luminosity with systematic background uncertainty of 20% for two search bins : ≥ 4 b-jets, $S_T > 600$ GeV (a), ≥ 4 b-jets, $S_T > 800$ GeV (b)

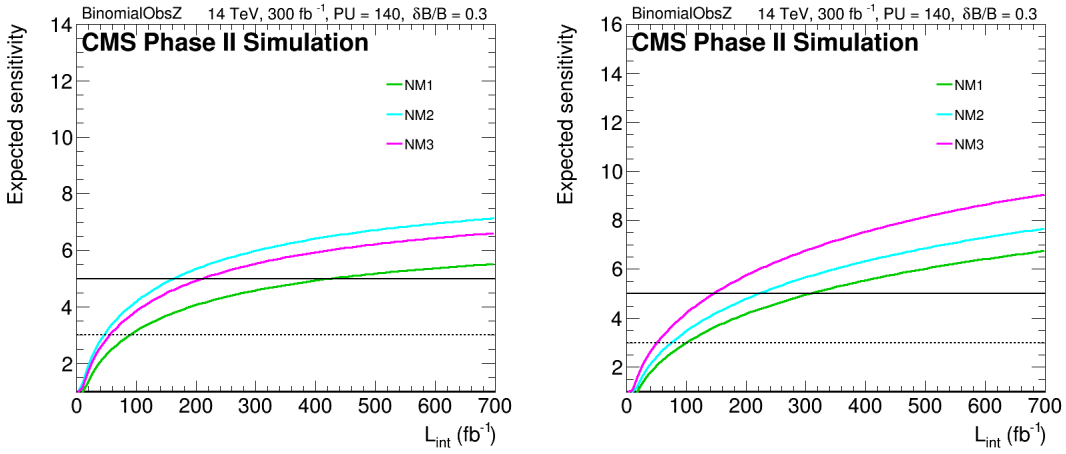

(a) (b)

Figure 15: Expected sensitivity as a function of luminosity with systematic background uncertainty of 30% for two search bins : ≥ 4 b-jets, $S_T > 600$ GeV (a), ≥ 4 b-jets, $S_T > 800$ GeV (b).

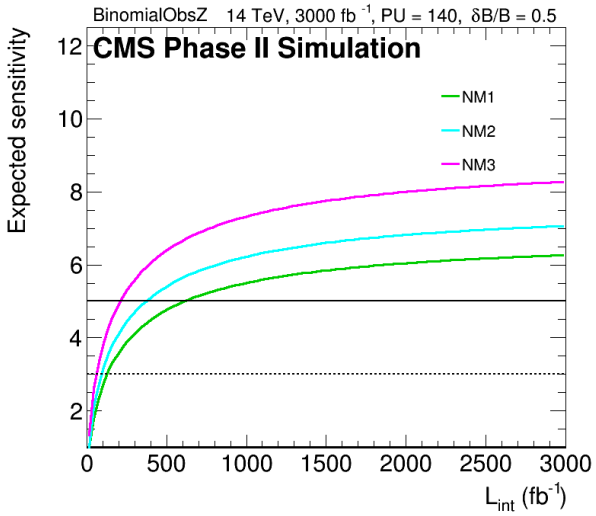

Figure 16: Expected sensitivity as a function of luminosity with systematic background uncertainty of 50% for search bin: ≥ 4 b-jets, $S_T > 800$ GeV.

Table 4: The event yields for the signal samples and several SM processes with 300 fb^{-1} at 14 TeV for 140 and 50 pileup.

Cut	**$t\bar{t}$**	**W/Z + jets**	**diboson**	**single top**	**BKG**	**NM1**	**NM2**	**NM3**
Preselection	159400	54615	5495	2082	221592	444	509	482
search bin: ≥3b-jet, $S_T > 600$ GeV								
≥3b-jet	14954	309	40	155	15459	198	275	208
H_T >1500	3845	64	13	31	3952	158	255	164
S_T>600	144	7	2	2	154	71	94	95
Lp<0.2	69	3	1	1	73	61	76	83
|Lp| < 0.2	42	1	0	0	44	56	67	76
|Lp|(50PU) < 0.2	39	1	0	0	40	57	66	83
search bin: ≥3b-jet, $S_T > 700$ GeV								
S_T>700	66	3	1	1	72	51	62	74
Lp<0.2	32	2	0	0	35	44	50	66
|Lp|<0.2	20	1	0	0	21	41	45	60
|Lp|(50PU) < 0.2	19	1	0	0	20	41	44	65
search bin: ≥3b-jet, $S_T > 800$ GeV								
S_T>800	31	2	1	0	34	35	39	57
Lp<0.2	16	1	0	0	18	30	32	52
|Lp|<0.2	10	1	0	0	11	28	28	48
|Lp|(50PU) < 0.2	9	0	0	0	10	28	28	49
search bin: ≥4b-jet, $S_T > 600$ GeV								
≥4b-jet	1926	16	4	17	1962	79	139	79
H_T >1500	608	4	1	3	617	64	131	64
S_T>600	21	0	0	0	22	29	47	38
Lp<0.2	10	0	0	0	10	25	38	33
|Lp|<0.2	6	0	0	0	6	23	33	30
|Lp|(50PU) < 0.2	6	0	0	0	7	23	33	33
search bin: ≥4b-jet, $S_T > 700$ GeV								
S_T>700	9	0	0	0	9	21	30	29
Lp<0.2	4	0	0	0	5	18	25	25
|Lp|<0.2	3	0	0	0	3	17	22	22
|Lp|(50PU) < 0.2	3	0	0	0	3	16	22	26
search bin: ≥4b-jet, $S_T > 800$ GeV								
S_T>800	4	0	0	0	4	14	19	22
Lp<0.2	2	0	0	0	2	12	16	20
|Lp|<0.2	1	0	0	0	1	11	14	18
|Lp|(50PU) < 0.2	2	0	0	0	2	11	14	19

5 Conclusion

Three full SUSY natural models were investigated for being discovered at LHC and HL-LHC in the CMS experiment. S_T and L_P were used as discriminating variables in the inclusive search with the single lepton in final state. Two pileup scenarios: 50 PU and 140 PU were compared and the analysis is concluded to be pileup independent. We compare two different methods of significance calculation and propose the most reliable one to be used. Next, an expected sensitivity as a function of systematic uncertainty was calculated. For two systematic uncertainties (lower and higher than in previous 8 TeV analysis) the dependence of the significance on the integrated luminosity was evaluated. It was investigated that with 30% background uncertainty NM1 is discoverable with integrated luminosity 300 fb^{-1}, NM2 with 250 fb^{-1} and NM3 already with 150 fb^{-1}.

References

[1] I. J. R. Aitchison, "Supersymmetry and the MSSM: An Elementary Introduction", arXiv:hep-ph/0505105

[2] CMS Collaboration, "Search for supersymmetry in final states with a single lepton, b-quark jets, and missing transverse energy in proton-proton collisions at sqrt(s) = 7 TeV", Phys. Rev. D 87(2013) 052006.

[3] CMS Collaboration, "Search for supersymmetry in pp collisions at sqrt(s) = 8 TeV in events with a single lepton, large jet multiplicity, and multiple b jets", Phys. Lett. B 733 (2014) 328.

[4] J. T. Linnemann, "Measures of Significance in HEP and Astrophysics", arXiv:physics/0312059